Analytical expression for thermal conductivity of heat pipe

Article *in* Applied Thermal Engineering · February 2016

DOI: 10.1016/j.applthermaleng.2016.02.042

3 authors, including:

A. Brusly Solomon
University of Pretoria
21 PUBLICATIONS **136** CITATIONS

SEE PROFILE

Applied Thermal Engineering 100 (2016) 462–467

Contents lists available at ScienceDirect

Applied Thermal Engineering

journal homepage: www.elsevier.com/locate/apthermeng

Analytical expression for thermal conductivity of heat pipe

A. Brusly Solomon [a], M. Sekar [a,*], S.H. Yang [b]

[a] Centre for Research in Material Science and Thermal Management, Department of Mechanical Engineering, Karunya University, Coimbatore 641114, India
[b] Department of Mechanical Engineering, Kyungpook National University, Deagu 702-701, South Korea

ARTICLE INFO

Article history:
Received 25 August 2015
Accepted 15 February 2016
Available online 23 February 2016

Keywords:
Thermal conductivity
Heat pipe
Dry machining
Analytical model
Thermal resistance
Lumped network analysis

ABSTRACT

An analytical expression is proposed to predict the thermal conductivity of a heat pipe based on the heat transport limit equations. The experimental results of thermal conductivity of heat pipe measured at different heat inputs are compared with the thermal conductivity obtained from the analytical expression and found to be reasonable in agreement. The thermal conductivity of heat pipe obtained from the heat transport limit equation is also compared with lumped thermal resistant network model. The proposed analytical model is computationally effective and simple, and can be applied to a variety of applications. It is also useful for design and computational analysis of embedded heat pipes for machining applications.

1. Introduction

Metal machining is the most important form of metal removal process in industries such as automotive, aerospace, mold and die, consumer products, etc. During the metal machining process, a large amount of heat is generated due to the plastic deformation of material at the tool – work interface [1]. Heat generation is also found considerable even with the machining of metal matrix composites due to their abrasive nature [1–3]. Though a substantial portion of the heat generated during machining is carried away by the chip, continuous removal of metal by the machine tool increases the temperature of the cutting tool, work piece and machine.

Removal of heat generated in metal cutting operations is one of the most critical issues focused by the industries as increase in temperature above the permitted range will be detrimental to product dimensional accuracy, surface finish, tool wear and performance of the machine tool. In a typical machining process, a flood of coolant fluid is applied over the tool – work interface to carry away the heat. The contentious effects of coolant applied to remove heat during machining are widely reported in literature [4,5]. The toxic additives added to the coolant to improve its performance during metal cutting makes disposal of the coolant costly as it pollutes the environment. Dry machining and near dry machining have been developed [5] as other options to conventional machining however, are practiced limitedly. Recently, the applications of heat pipe to remove heat from turning tools, milling cutters [6–10], and drilling tools [11,12] are reported and look promising.

Heat pipes are passive heat transfer devices that can successfully transfer large amounts of heat. The robust and simple tubular structure with no moving parts makes the heat pipe a perfect choice to embed with rotating milling cutters. Recently, experimental [6–8,11,13] and numerical [6,7,11,14,15] studies are carried out to analyze the performance of heat pipe embedded in cutting tools. Zho et al. [14] performed an experimental study to analyze the feasibility and efficiency of heat pipe embedded drills by placing a heat pipe in the center of the drill with an evaporator positioned near the tip of the tool. A significant reduction in tool temperature is reported with the use of heat pipe embedded tools. It is also noticed that the prediction of maximum temperature in the tool along the rake face is an important parameter because of its influence on the tool life and quality of the machined part [2]. Numerical studies have gained more importance since measuring temperatures of the rotating cutting tool [16] is difficult [6,7]. However, these studies are complicated due to the non-linearity present in the equations governing vapor and liquid flow in a heat pipe. Shukla et al. [17] introduced an analytical model to determine the heat transport limit of a micro heat pipe considering capillary limit. Though several assumptions such as treating heat pipe as a material with high thermal conductivity [7,11], constant temperature cylinder [15], ignoring the phase change mechanism [18] etc., simplified the numerical solution, a more focused approach is required for the improvement of results. Hence, the approach of analytically modeling the thermal conductivity of a heat pipe is timely essential to find the temperature of the tool and is the focus in this study.

* Corresponding author. Tel.: +91 422 2614430; fax: +91 422 2615615.
E-mail address: mailtosekar@gmail.com (M. Sekar).

http://dx.doi.org/10.1016/j.applthermaleng.2016.02.042
1359-4311/

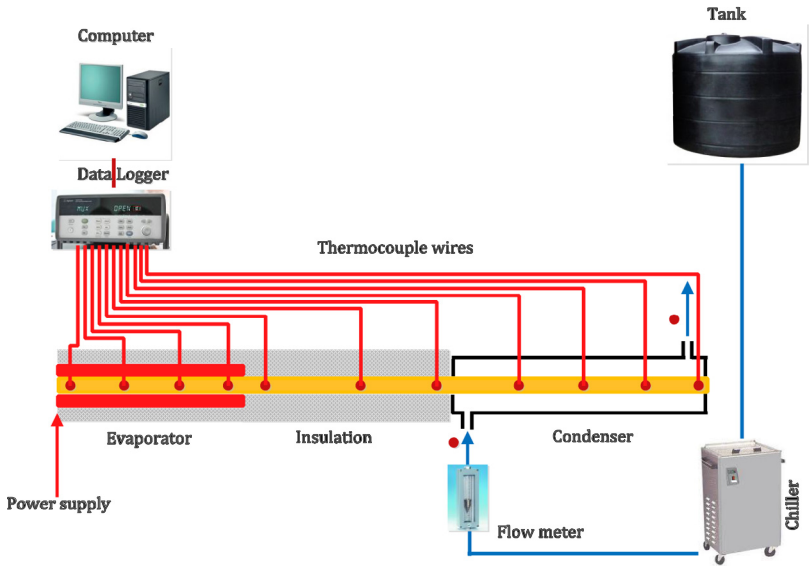

Fig. 1. View of experimental set up.

Thermal conductivity is an important parameter to determine the temperature variation between the evaporator and condenser sections of a heat pipe. In this direction, no report is available in the open literatures to the best of authors' knowledge. In the model proposed, the heat transport capacity of the heat pipe is assumed equal to the heat conducted by the heat pipe. Heat transport capacity of the heat pipe is estimated by comparing the capillary pressure generated by the wick structure and pressure losses that occur during vapor and liquid flow through the wick structure. Thermal conductivity of the heat pipe estimated by using Fourier law of heat conduction and lumped thermal resistance network model are compared with experimental measurements. Development of such analytical models will enable saving of a significant amount of experimental effort, computational cost and time.

2. Experimental methods

The proposed experimental test set up comprises of a test section, chiller and data acquisition system (Fig. 1). A straight copper tube of outer diameter 19 mm and length 350 mm forms the test section of the heat pipe. The corresponding lengths of the evaporator, adiabatic and condenser sections are 100, 100 and 150 mm, respectively. Four layers of copper screen mesh of wire diameter 80 μm and porosity 0.63 is used to fabricate a wick structure of thickness 1 mm. The wick structure is fixed to the inner wall of heat pipe by a spring support. The heat pipe is charged with 12 ml of DI water (deionized water), which is sufficient to saturate the complete wick structure.

The experimental setup consists of an electrical resistant heater having a maximum power input of 800 W to supply heat to the evaporator section. T-type (OMEGA) thermocouples with an uncertainty of ±0.2 °C are used to measure the wall temperatures of the heat pipe and the thermocouples are welded on the wall of heat pipe in the positions as shown in Fig. 2. Further, a thin layer of thermal interface material (TIM) is applied to minimize the heat resistance between surfaces of heater and evaporator sections of the heat pipe. A 40 mm thick glass wool with the thermal conductivity of 0.04 W/m-K is wound around the heater to reduce heat loss to the surroundings.

The condenser sector of the heat pipe is made of acrylic tube. Water from the reservoir is passed through the chiller and is supplied to the cooling jacket at a flow rate of 350 ml/min. The flow rate of the coolant is controlled using a calibrated flow meter having an uncertainty of ±3%. The temperature of the coolant is maintained at 22 ± 0.5 °C and the inlet and outlet cooling water temperature are measured using two OMEGA T-type thermocouples with uncertainty of ±2 °C. The entire experimental setup is placed horizontally with the help of a level indicator. Tests are carried out with heat inputs at the evaporator varying between 50 and 300 W. The heat pipe is allowed to reach a steady state and the temperature data are recorded over a time interval of 30 s.

The heat transported by the heat pipe under different heat loads is calculated by Newton law of cooling: $Q_t = \dot{m} \times C_p \times \Delta T$, where, $\dot{m}$ is the mass flow rate of coolant (water), C_p is the specific heat of coolant, ΔT is the temperature difference between outlet and inlet of the coolant.

The experimental thermal conductivity of the heat pipe obtained by the Fourier heat conduction equation is shown below

$$k_{eff} = Q \frac{L_{eff}}{A \Delta T} \tag{1}$$

where, Q is the heat transfer rate, ΔT is the temperature difference between the evaporator and condenser and L_{eff} is the effective length of heat pipe. The effective length of the heat pipe is expressed as

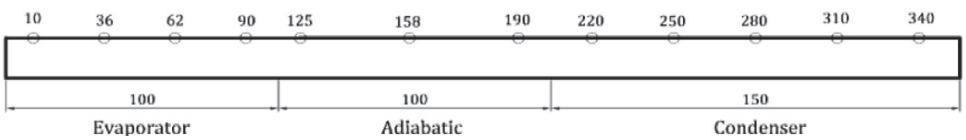

Fig. 2. Thermocouple position of heat pipe.

Table 1
Uncertainties in the measurement.

S. No	Heat input (W)	Uncertainty (%)		
		Heat flux	Resistance	Thermal conductivity
1	50	6.87	6.89	6.87
2	100	6.53	6.55	6.54
3	150	4.30	4.32	4.31
4	200	4.04	4.05	4.04
5	250	3.54	3.56	3.55
6	300	3.65	3.66	3.65

$$L_{eff} = \left(\frac{L_e + L_{con}}{2}\right) + L_a \tag{2}$$

where, L_e, L_a and L_{con} are the lengths of evaporator, adiabatic and condenser sections of heat pipe.

The uncertainties present in the estimation of heat transfer, heat flux, resistance and thermal conductivity of the heat pipes are found using the equations (3–6).

$$\frac{\Delta Q}{Q} = \sqrt{\left(\frac{\Delta m}{m}\right)^2 + \left(\frac{\Delta t}{t}\right)^2} \tag{3}$$

$$\frac{\Delta q}{q} = \sqrt{\left(\frac{\Delta Q}{Q}\right)^2 + \left(\frac{\Delta A}{A}\right)^2} \tag{4}$$

$$\frac{\Delta R}{R} = \sqrt{\left(\frac{\Delta Q}{Q}\right)^2 + \left(\frac{\Delta T}{T}\right)^2} \tag{5}$$

$$\frac{\Delta K}{K} = \sqrt{\left(\frac{\Delta q}{q}\right)^2 + \left(\frac{\Delta(\Delta T_{hp})}{\Delta T}\right)^2 + \left(\frac{\Delta L}{L}\right)^2} \tag{6}$$

The uncertainties in the measurement of heat flux, resistance and thermal conductivity measurement are presented in Table 1.

3. Theoretical calculation

Heat pipes are two phase heat transfer devices that transport a large amount of heat through a small cross section with extremely small temperature drop. The heat transport is limited by the capillary force, which is essential for the continuous operation of heat pipes. Heat transport limitations are classified as capillary limit, sonic limit, viscous limit, entrainment limit and boiling limit based on the properties of wick, working fluid and geometric structure. The capillary limit is considered to be most fundamental and basic limit because the capillary pressure differences between the liquid–vapor interface in the evaporation and condensing section determines the successful heat transport in the heat pipe. Hence, in this study, the thermal conductivity of the heat pipe is estimated with the use of the capillary limit.

3.1. Thermal conductivity estimation in the axial direction

The thermal conductivity of the heat pipe is calculated by assuming the heat transport limit of the heat pipe equal to the heat conducted by the heat pipe. Heat transport limit mainly depends on the capillary pressure generated by the wick structure and the pressure losses generated due to the phase change of working fluid, friction losses due to vapor and liquid flow, etc. The heat pipe functions efficiently when the net capillary pressure between the evaporator and condenser is greater than the pressure losses occurring throughout the vapor and liquid flows. Otherwise, dry-out will occur at the evaporator due to insufficient liquid supply.

The capillary limit can be calculated by equating the capillary pressure to pressure losses as shown in equation (7).

$$\Delta P_{c,m} = \Delta P_v + \Delta P_l + \Delta P_{Ph,e} + \Delta P_{Ph,c} + \Delta P_+ + \Delta P_{ll} \tag{7}$$

where,

$\Delta P_{c,m}$ = maximum capillary pressure difference generated within capillary wicking structure between wet and dry points
ΔP_v = sum of inertial and viscous pressure drops occurring in vapor phase
ΔP_l = sum of inertial and viscous pressure drops occurring in liquid phase
$\Delta P_{Ph,e}$ = pressure gradient across phase transition in evaporator
$\Delta P_{Ph,c}$ = pressure gradient across phase transition in condenser
ΔP_+ = normal hydrostatic pressure drop
ΔP_{ll} = axial hydrostatic pressure drop

The following assumptions are made to calculate the capillary pressure:

a) In vapor phase, the viscous pressure losses are taken into account and the inertial effects are neglected.
b) The vapor phase transition losses are neglected.
c) The vapor flow is assumed to be one dimensional along the axial direction of the heat pipe.

With the above assumptions, Eqn. (7) can be written as

$$\frac{2\sigma\cos\theta}{r_c} = \frac{16\mu_v L_{eff} Q_T}{2r_{h,v}^2 A_v \rho_v h_{fg}} + \frac{\mu_l L_{eff} Q_T}{K A_\omega \rho_l h_{fg}} + \rho_l g d_v \tag{8}$$

As the maximum heat transferred is equal to heat conducted by the heat pipe the capillary limit Q_T can be expressed as:

$$Q_T = k_{eff} A \frac{\Delta T}{L_{eff}} = \left(\frac{2\sigma\cos\theta}{r_c} - \rho_l g d_v\right)\left[\frac{16\mu_v L_{eff}}{2r_{h,v}^2 A_v \rho_v h_{fg}} + \frac{\mu_l L_{eff}}{K A_\omega \rho_l h_{fg}}\right]^{-1} \tag{9}$$

where K is the permeability of the wick structure $K = \dfrac{d_\omega^2 \varepsilon^3}{122(1-\varepsilon)^2}$ (10)

Rearranging Eqn. (9), the thermal conductivity of the heat pipe is obtained:

$$k_{eff} = \frac{h_{fg}\left(\dfrac{2\sigma\cos\theta}{r_c} - \rho_l g d_v\right)}{A\Delta T\left[\dfrac{16\mu_v}{2r_{h,v\rho_v A_v}^2} + \dfrac{\mu_l}{K A_\omega \rho_l}\right]} \tag{11}$$

The above equation enables the calculation of the thermal conductivity of the heat pipe based on thermo-physical properties of working fluids and wick properties. The thermo-physical properties of the working fluid at different vapor temperatures of heat pipe corresponding to this study are listed in Table 2 [19].

3.2. Lumped thermal resistance analysis

The overall thermal resistance of the heat pipe calculated using lumped thermal resistance network model [20,21] is shown in Fig. 3. In this model, the overall resistance of the heat pipe is given by

Table 2
Thermo-physical properties of working fluid.

Vapor temperature (°C)	Thermal conductivity (W/m-K)		Surface tension (N/m)	Latent heat (KJ/kg)	Viscosity ×10^{-6} (N-s/m^2)		Density (kg/m^3)	
	Copper	Liquid			Liquid	Vapor	Liquid	Vapor
37.8	400	0.6235	0.06985	2448.59	690	9.57	993.7	0.0473
45.8	397.9	0.6364	0.0687	2392.56	597	9.903	990.2	0.0740
51.9	398.5	0.6447	0.06747	2377.88	539	10.16	987.1	0.0981
57.3	398	0.6507	0.06653	2364.89	488	10.38	984.6	0.1195
61.3	397.5	0.6521	0.0658	2355.18	456	10.55	982.5	0.1407
65	397.83	0.6582	0.0652	2346.02	435	10.69	980.9	0.1709

$$R_{total} = R_{p,e} + R_{w,e} + R_v + R_{p,con} + R_{w,con} + \frac{1}{R_{p,a}} + \frac{1}{R_{w,a}} \tag{12}$$

The thermal resistances due to the pipe wall in the evaporator ($R_{p,e}$), liquid-wick at evaporator ($R_{w,e}$), liquid-wick at condenser ($R_{w,con}$) and pipe wall in the condenser ($R_{p,con}$) are

$$R_{p,e} = \frac{\ln\left(\frac{d_o}{d_i}\right)}{2\pi L_e k_p}, R_{w,e} = \frac{\ln\left(\frac{d_i}{d_v}\right)}{2\pi L_e k_{wick}}, R_{w,con} = \frac{\ln\left(\frac{d_i}{d_v}\right)}{2\pi L_{con} k_{wick}}, R_{p,con} = \frac{\ln\left(\frac{d_o}{d_i}\right)}{2\pi L_{con} k_p} \tag{13}$$

where, the effective thermal conductivity of the wick structure is

$$k_{wick} = k_l \left[\frac{(k_l + k_w) - (1-\varepsilon)(k_l - k_w)}{(k_l + k_w) + (1-\varepsilon)(k_l - k_w)}\right] \tag{14}$$

The thermal resistance of the vapor flow, R_v is determined by

$$R_v = \frac{T_v (P_{v,e} - P_{v,con})}{\rho_v h_{fg} q_{con}} \tag{15}$$

where, $P_{v,e}$ and $P_{v,con}$ are the saturation vapor pressures at corresponding vapor temperature at the evaporator and condenser, respectively. The vapor temperatures at the evaporator and condenser sections of heat pipe are calculated by Fourier heat conduction equation.

Summing all the individual resistances (Eqn. 12) the thermal conductivity of the heat pipe is estimated as

$$k_{eff} = \frac{L_{eff}}{R_{total}} \tag{16}$$

4. Results and discussion

In this study, the heat transfer characteristics of heat pipe with screen mesh wick are analyzed. The wall temperature at different positions of the heat pipe is measured. Fig. 4 shows the average wall temperature of the heat pipe at the evaporator, vapor and condenser sections at different heat inputs. It can be inferred that the wall temperatures at various sections of the heat pipe increase linearly with heat input given by external source. Further, it is observed that the temperature at the evaporator section is higher than the temperatures at the vapor and condenser sections, which confirm the desired functionality of the heat pipe. The wall temperature of the heat pipe at the evaporator, adiabatic and condenser sections at various heat loads (50–300 W) are found to vary between 57 and 120, 37 and 65, and 29 and 42 °C, respectively. As a result, the temperature difference (ΔT) between the evaporator and condenser of heat pipe also increases linearly with heat inputs (Fig. 5), which ensures proper functioning and steady transfer of heat in the heat pipe. The higher ΔT of 80 °C observed with 300 W power input is due to the increased wall temperature at the evaporator section (Fig. 4). The increase in wall temperature may be the result of the partial dry out condition at the evaporator section. The total resistance of heat pipe estimated by the equation $R = \Delta T/Q$, (where Q is the heat transferred by the heat pipe) exponentially decreases with the increasing heat inputs as shown in Fig. 6. As the heat input

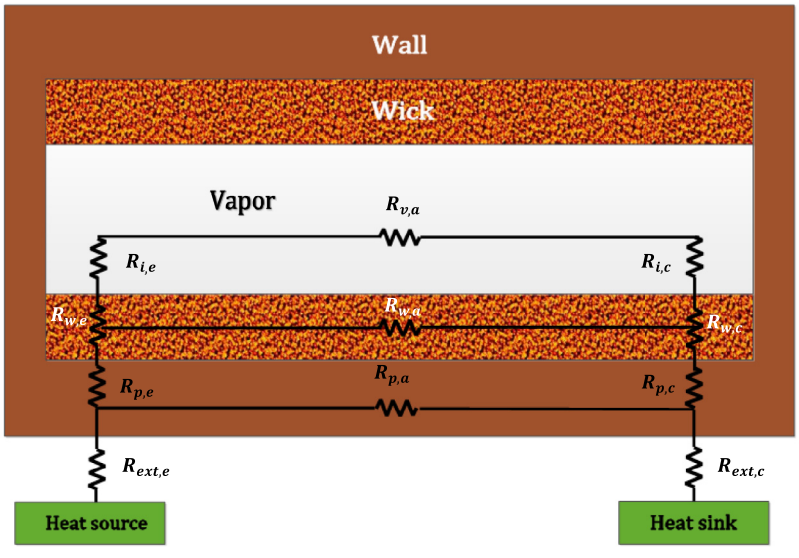

Fig. 3. Lumped thermal resistance network.

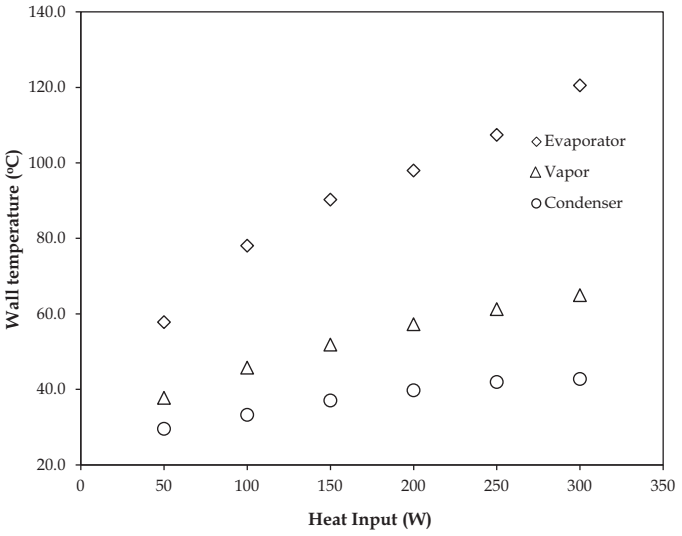

Fig. 4. Temperature responses of heat pipe at different heat inputs.

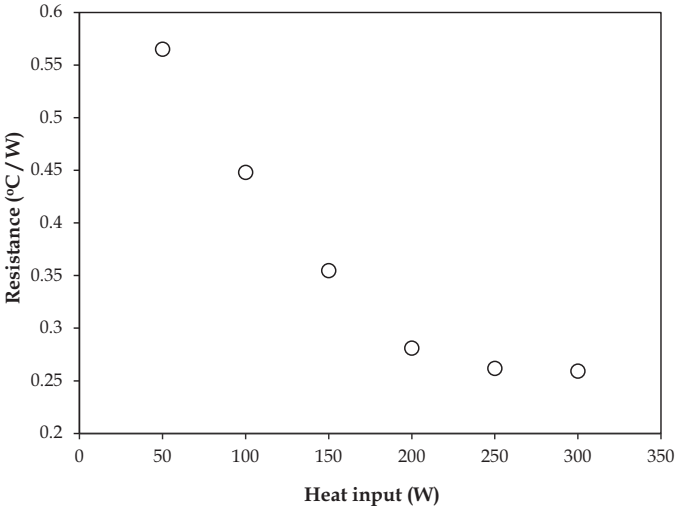

Fig. 6. Thermal resistance of heat pipe at different heat inputs.

increases from 50 to 250 W, the thermal resistance reduces from 0.56 to 0.25 °C/W and remains constant until 300 W. This observation shows that further increase in heat input does not contribute to the decrease in thermal resistance since the heat transfer limit corresponding to the power level has already been reached. It can be noticed that the effect of heat input on the thermal resistance is significant at low power levels compared to higher power levels.

The thermal conductivity of the heat pipe is calculated (Eqn. 1) and compared with the analytical results (Eqn. 11). Fig. 7 shows the thermal conductivity of the heat pipe obtained through experimental, proposed and lumped models at various heat inputs. The results show a similar pattern on the thermal conductivity estimated by experiment, lumped model and proposed model. The proposed model correctly predicts the increase in thermal conductivity with the increase in the heat input and the same is validated experimentally. Further, it is noticed that the proposed model over predicts the thermal conductivity of experimental and lumped model at lower heat inputs. The present model is developed based on the capillary limit of the heat pipe, which is the maximum heat transfer limit of the heat pipe. The experimental results are consistent at higher heat inputs as the capillary limit is accountable for maximum heat transport. The deviations at low power inputs can further be reduced by considering the viscous limit, sonic limit etc., in addition to the capillary limit. Though a deviation between the proposed model and experiment is noticed at lower heat input, the thermal conductivity calculated with the experiment and the proposed model is comparable at higher heat inputs. The maximum thermal conductivity obtained using the analytical model and experiment is about 18,290 W/m-K. A similar value of thermal conductivity of 15,000–30,000 W/m-K was reported in [18]. Though experimental and lumped models are also comparable at lower heat inputs, a marginal deviation is seen at higher heat inputs. This variation is mainly attributed to the difference in vapor pressure between the evaporator and condenser of heat pipe (Equation 15), and the variation in thermo-physical properties of working fluids. In the present study, the vapor pressure at the evaporator and condenser of heat pipe is taken at corresponding saturation vapor temperature at the corresponding sections of the heat pipe. The vapor temperature is calculated based on the heat conduction equation, which is derived from the wall temperature of the heat pipe. Hence, in order to reduce the thermal conductivity variation between the

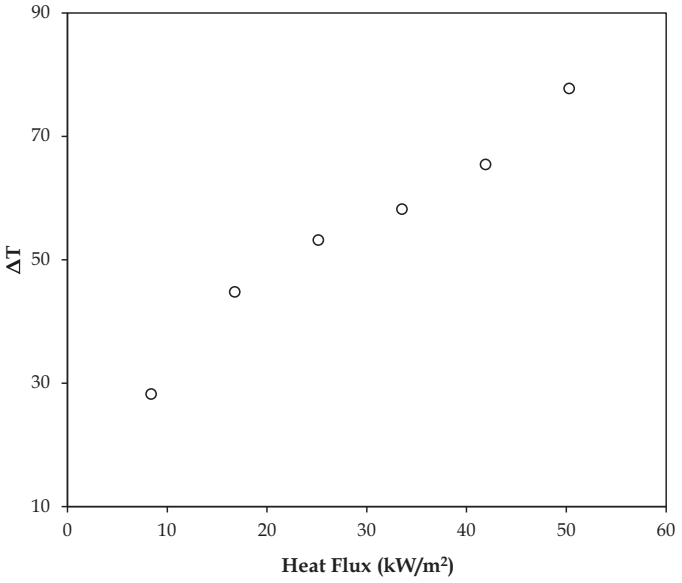

Fig. 5. Temperature difference of heat pipe at different heat fluxes.

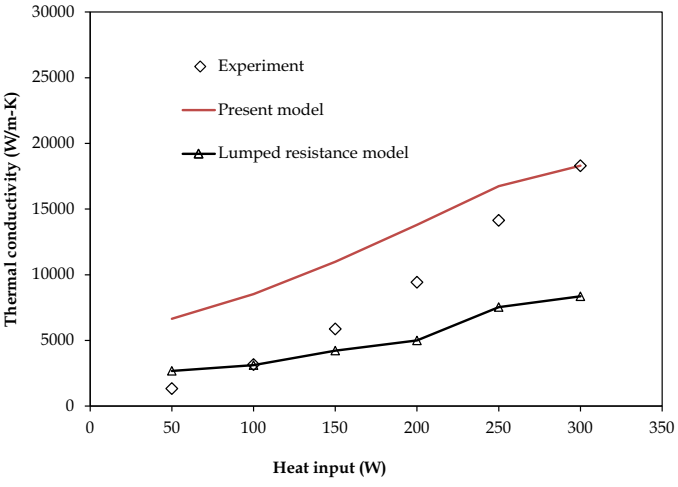

Fig. 7. Thermal conductivity of heat pipe at different heat inputs.

experimental and lumped models, accurate pressure measurements are essential, which is beyond the scope of the present work.

5. Conclusions

An analytical expression to estimate the thermal conductivity of a heat pipe is derived and the same is validated with experimental results. A copper/water heat pipe with screen mesh wick is fabricated for this purpose and tested under various heat input conditions. The maximum thermal conductivity obtained using the analytical model (18,290 W/m-K) shows reasonably good agreement with the experimental thermal conductivity. The influence of temperature difference between the evaporator and condenser sections and thermo physical properties of the working fluid in enhancing the thermal conductivity is evident as the thermal conductivity is enhanced from 8532 to 18,294 W/m^2-K for the increase of heat input from 50 to 300 W. The generalized model proposed in this work can easily be extended to compute thermal conductivities of heat pipes made with different types of working fluids and wick materials. Prior estimation of thermal conductivity of heat pipes through this analytical method can make numerical studies faster. This model is also useful in predicting the cutting tool temperatures that are otherwise difficult to measure in machining applications carried out with rotating tools such as drills, end mills etc., This model can effectively be used in the design of special types of cutting tools embedded with heat pipes for the effective removal of heat generated in machining.

Acknowledgements

The authors gratefully acknowledge the critical reviews carried out by the anonymous reviewers toward the improvement of the article.

Nomenclature

A	Area [m^2]
d	Diameter [m]
g	Gravitational force [m/s^2]
h	Heat of vaporization [J/kg-K]
L	Length [m]
m	Mass flow rate [kg/s]
k	Thermal conductivity [W/m-K]
K	Permeability
P	Pressure [Pa]
ΔP	Pressure difference
q	Heat flux [W/m^2]
Q	Heat transfer rate [W]
R	Resistance [°C/W]
r	Radius [m]
T	Temperature [°C]
σ	Surface tension [N/m]
μ	Viscosity [N-s/m^2]
ρ	Density [kg/m^3]
ε	Porosity
ΔT	Temperature difference between the vapor and condenser
Δt	Temperature difference between the outlet and inlet of the coolant

Subscripts

a	Adiabatic
c	Critical
con	Condenser
eff	Effective
e	Evaporator
f,l	Liquid
i	Inner
o	Outer
p	Wall
s	Supplied
t	Transferred (experimental)
T	Transported (analytical)
v	Vapor
ω	Wick

References

[1] R. Sekhar, T.P. Singh, Mechanisms in turning of metal matrix composites: a review, J. Mater. Res. Technol. 4 (2) (2015) 197–207.
[2] N.A. Abukhshim, P.T. Mativenga, M.A. Sheikh, Heat generation and temperature prediction in metal cutting: a review and implications for high speed machining, Int. J. Mach. Tools Manuf. 46 (2006) 782–800.
[3] P. Majumdar, R. Jayaramachandran, S. Ganesan, Finite element analysis of temperature rise in metal cutting processes, Appl. Therm. Eng. 25 (2005) 2152–2168.
[4] P. Semanova, M. Kucera, Health effects from occupational exposure to metalworking fluid mist, Key Eng. Mater. 581 (2014) 112–118.
[5] P.S. Sreejith, B.K.A. Ngoi, Dry machining: machining of the future, J. Mater. Process. Technol. 101 (2000) 287–291.
[6] R.Y. Chiou, L. Lu, J.S.J. Chen, M.T. North, Investigation of dry machining with embedded heat pipe cooling by finite element analysis and experiments, Int. J. Adv. Manuf. Technol. 31 (2007) 905–914.
[7] J. Liu, Y.K. Chou, Cutting tool temperature analysis in heat-pipe assisted composite machining, J. Manuf. Sci. Eng. 129 (2007) 902–910.
[8] L. Zhu, S.-S. Peng, C.-L. Yin, T.-C. Jen, X. Cheng, Y.-H. Yen, Cutting temperature, tool wear, and tool life in heat-pipe-assisted end-milling operations, Int. J. Adv. Manuf. Technol. 72 (2014) 995–1007.
[9] L. Zhu, T.-C. Jen, Y.-H. Yen, X.-L. Kong, Feasibility and effectiveness of heat pipe cooling in end milling operations: thermal, structural static, and dynamic analyses: a new approach, J. Manuf. Sci. Eng. 133 (2011) 054503.
[10] Y. Quan, Q. Mai, Investigation of the cooling effect of heat pipe-embedded cutter in dry machining with different thermal conductivities of cutter/work piece materials and different cutting parameters, Int. J. Adv. Manuf. Technol. 79 (2015) 1161–1169.
[11] T.C. Jen, G. Gutierrez, S. Eapen, J. Manjunathaiah, Investigation of heat pipe cooling in drilling applications. Part I: preliminary numerical analysis and verification, Int. J. Mach. Tools Manuf. 42 (2002) 643–652.
[12] L. Zhu, T.-C. Jen, Y.-B. Liu, J.-W. Zhao, W.-L. Liu, Y.-H. Yen, Cutting tool life analysis in heat-pipe assisted drilling operations, J. Manuf. Sci. Eng. 137 (2015) 011008.
[13] L. Zhu, T.-C. Jen, C.-L. Yin, X.-L. Kong, Y.-H. Yen, Experimental analyses to investigate the feasibility and effectiveness in using heat pipe-embedded drills, Int. J. Adv. Manuf. Technol. 58 (2012) 861–868.
[14] L. Zhu, T.-C. Jen, C.-L. Yin, X.-L. Kong, Y.-H. Yen, Investigation of the feasibility and effectiveness in using heat pipe-embedded drills by finite element analysis, Int. J. Adv. Manuf. Technol. 64 (2013) 659–668.
[15] Y.-B. Liu, L. Zhu, T.-C. Jen, J.-W. Zhao, Y.-H. Yen, Numerical analyses to investigate the feasibility and effectiveness in using heat pipe embedded end mills, Strojniški Vestnik 58 (3) (2012) 213–220.
[16] G. Le Coz, M. Marinescu, A. Devillez, D. Dudzinski, L. Velnom, Measuring temperature of rotating cutting tools: application to MQL drilling and dry milling of aerospace alloys, Appl. Therm. Eng. 36 (2012) 434–441.
[17] K.N. Shukla, Heat transfer limitation of a micro heat pipe, J. Electron. Packag. 121 (2009) 024502.
[18] J. Legierski, B. Wiecek, G.D. Mey, Measurements and simulations of transient characteristics of heat pipes, Microelectron. Reliab. 46 (1) (2006) 109–115.
[19] A. Faghri, Heat Pipe Science and Technology, Taylor Francis, USA, 1995.
[20] G.P. Peterson, An Introduction to Heat Pipes: Modeling, Testing, and Applications, Wiley, 1994.
[21] C. Ferrandi, F. Iorizzo, M. Mameli, S. Zinna, M. Marengo, Lumped parameter model of sintered heat pipe: transient numerical analysis and validation, Appl. Therm. Eng. 50 (2013) 1280–1290.